Tuning the Dielectric & Optical Properties of BiFeO$_3$ Thin Films

M. Adnan Naseer[1], Attia Awan[2], Saira Riaz[3], Shahid Atiq[4]
and *Shahzad Naseem[5]

[1), 2), 3), 4), 5)] *Centre of Excellence in Solid State Physics, University of the Punjab, Lahore, Pakistan*
[5] *shahzad.cssp@pu.edu.pk*

ABSTRACT

Bismuth iron oxide belongs to the class of materials that exhibits simultaneous presence of ferromagnetic and ferroelectric properties. However, synthesis of phase pure bismuth iron oxide presents some difficulties due to volatile nature of bismuth oxide. In order to overcome this difficulty, bismuth iron oxide thin films are prepared with variation in Bi/Fe ratio as 0.9, 0.95, 1.0, 1.05, 1.10, 1.15 and 1.20. XRD results confirm the formation of phase pure bismuth iron oxide in Bi/Fe ratio 1.0-1.10, while contribution from bismuth rich phase is observed as Bi/Fe ratio is increased to 1.20. Dielectric constant and tangent loss decrease as frequency of applied field increases and become constant at high frequencies. Dispersion in dielectric constant can be explained on the basis of Koop's theory based on Maxwell Wagner two-layered model. According to this model, specimen is composed of two layers, grains and grain boundaries. Grains are more conducting as compared to grain boundaries. At low frequencies, role of grain boundaries dominates resulting in high dielectric constant. At high frequencies, the role of grains dominates as a result of which the dielectric constant decreases at high frequencies along with decrease in tangent loss at high frequencies. Films show high transmission in the visible and infrared region with band gap in the range of 2.42eV-2.54eV. High refractive index of the films indicates compact structure of the films.

1. INTRODUCTION

During the last many years, numerous multiferroics have been identified including Cr$_3$B$_7$O$_{13}$Cl, BiMnO$_3$, NdMn$_2$O$_5$, HoMnO$_3$, LuMnO$_3$ etc. (Tripathy et al. 2013) but bismuth iron oxide (BiFeO$_3$, BFO) is one of the novel categories of materials which shows existence of correlated electric and magnetic orders (Arora et al. 2014). BFO has Neel antiferromagnetic and Curie ferroelectric temperatures of 643K and 1103K, respectively. These materials play substantial role in developing systems with large magneto electric coupling and offer applications in spintronics related materials and devices, sensors, etc. (Arora et al. 2014, Zhao et al. 2013). BFO possesses rhombohedrally distorted perovskite structure. 6s^2 lone pair of electrons on Bi site contribute to ferroelectric nature (Mazumder et al. 2006). Ferromagnetism in BFO is because of the presence of Fe^{3+} cations (Mazumder et al. 2006, Arora et al. 2014).

Due to coupling of electric and magnetic polarization these materials have properties that have not been explored yet (Salje et al. 1990). BFO has five following

main phases $BiFeO_3$, $Bi_2Fe_4O_9$, $Bi_3Fe_5O_{12}$, $Bi_4Fe_2O_9$ and $Bi_{46}Fe_2O_{72}$. But phase pure $BiFeO_3$ has very narrow temperature stability range (Riaz et al. 2015). Both bismuth and iron exhibit affinity to oxygen anions. This effect results in mixed phases. Perejon et al. (2002) have made efforts to synthesize bulk $BiFeO_3$ but could not eliminate the contribution from $Bi_{24}Fe_2O_{39}$ and $Bi_2Fe_4O_9$. Palkar et al. (2009) used solid-state reaction method in order to prepare pure BFO ceramic but they did not observe hysteresis loop at room temperature due to low resistivity. Yan et al. (2014) prepared BFO nanoparticles by hydrothermal method and studied the structural and phase transition.

For obtaining phase pure $BiFeO_3$, Bi/Fe ratio was varied in the present work. Films were prepared using sol-gel and spin coating method. Variations in optical and dielectric properties are linked with phase variations due to changes in Bi/Fe ratio.

2. EXPERIMENTAL DETAILS

BFO thin films with variation in Bi/Fe ratio 0.9, 1.0, 1.10 and 1.20 were synthesized using $Bi(NO_3)_3.5H_2O$ and $Fe(NO_3)_3.9H_2O$. Ethylene glycol was used as solvent. $Bi(NO_3)_3.5H_2O$ and $Fe(NO_3)_3.9H_2O$ were dissolved in the solvent and were heated at 80°C to ensure sol formation. Detailed steps for sol synthesis have been reported by Riaz et al. 2014. The sols were then deposited on Cu substrates. Cu substrates were thoroughly cleaned by etching with diluted HCl and by keeping in ultrasonic bath for 15 minutes in acetone and IPA (Asghar et al. 2006a,b). Phase analysis was carried out using Bruker D8 Advance X-ray Diffractometer. For dielectric and optical measurements 6500B Precision Impedance analyzer and JA Woolam M-2000 variable angle spectroscopic ellipsometer were used, respectively.

3. RESULTS AND DISCUSSIONS

X-ray diffraction patterns of BFO thin films with variation in Bi/Fe ratio synthesized by sol gel method are shown in the Fig 1. Bi/Fe ratio was varied as 0.9, 1.0, 1.10 and 1.20. It can be seen in Fig. 1 that with Bi/Fe ratios of 1.0 and 1.10 phase pure $BiFeO_3$ was obtained. With Bi/Fe ratio 1.20 inclusion of bismuth rich phase was also observed. Crystallinity of BFO thin films increases as Bi/Fe ratio =1.10. At Bi/Fe ratio =1.20 decrease in crystalline order is attributed to presence of mixed $BiFeO_3$ and $Bi_{24}Fe_2O_{39}$ phases. It can be seen in XRD patterns of Fig. 1 that both high and low Bi/Fe ratio resulted in presence of non-perovskite structures in bismuth iron oxide thin films while only Bi/Fe ratios of 1.0 and 1.10 resulted in phase pure $BiFeO_3$.
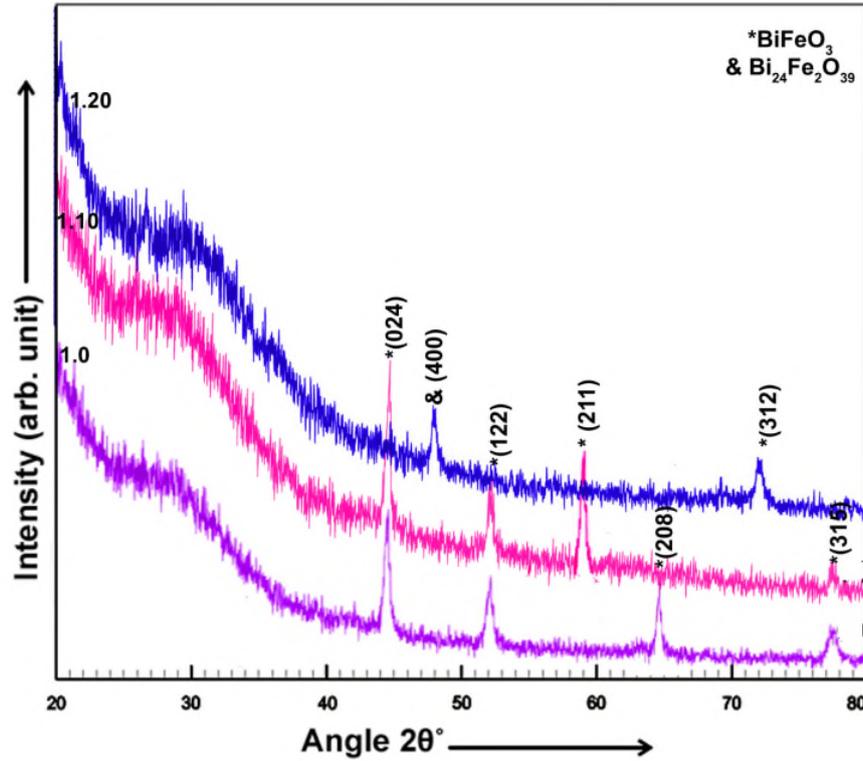
Fig.1 XRD patterns for BiFeO$_3$ thin films

Crystallite size (*t*) (Cullity 1956) and dislocation density (*δ*) were calculated using Eqs. 1-2 (Kumar et al. 2011).

$$t = \frac{0.9\lambda}{B\cos\theta} \tag{1}$$

$$\delta = \frac{1}{t^2} \tag{2}$$

Where, *θ* is the diffraction angle, λ is the wavelength (1.5406Å) and *B* is Full Width at Half Maximum. Crystallite size increases up to Bi/Fe ratio of 1.10 (Fig. 2). Whereas, crystallite size decreases at Bi/Fe ratio 1.20. Conversely, dislocation density decreases. Initially, reduction in crystallite size at Bi/Fe ratio 1.0 is associated with phase transformation from mixed bismuth deficient phases to phase pure BiFeO$_3$. Increase in crystallite size and decrease in dislocation density at Bi/Fe ratio 1.10 is indicative of strengthening of BiFeO$_3$ phase. Decrease in crystallite size accompanied by increase in dislocation density at high dopant concentration is associated with presence of BiFeO$_3$ and Bi$_{24}$Fe$_2$O$_{39}$ mixed phases (Fig. 1).
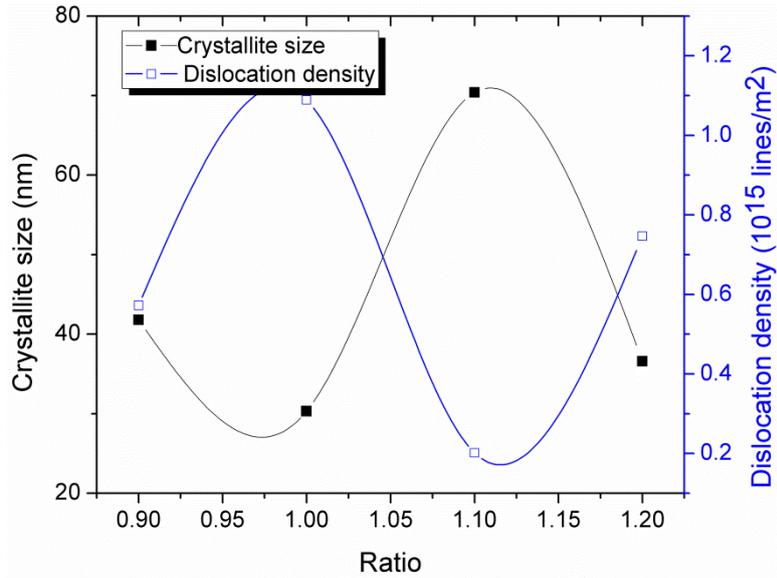
Fig. 2 Crystallite size and dislocation density for bismuth iron oxide thin films plotted as a function of Bi/Fe ratio

Dielectric constant (ε) and tangent loss (*tan δ*) were determined using Eqs. 3 and 4 (Barsoukov and Macdonald 2005).

$$\varepsilon = \frac{Cd}{\varepsilon_o A} \tag{3}$$

$$\tan \delta = \frac{1}{2\pi f \varepsilon_o \varepsilon \rho} \tag{4}$$

Where, C is the capacitance of films, d is the film thickness, ε_o is the permittivity of free space, A is the area, f is the frequency and ρ is the resistivity. Fig. 3 shows that dielectric constant and tangent loss displays normal dispersion behavior. At high frequencies only electronic polarization contributes while at low frequencies along with electronic, ionic interfacial polarization also contributes (Liu et al. 2007). This leads to high dielectric constant at low frequencies. Whereas, at high frequencies due to decrease in polarization dielectric constant and tangent loss both decrease. In addition, accumulation of ions at the grain boundaries at low frequencies leads to high resistance and hence dielectric constant. Whereas, at high frequencies, grains are more active and they exhibit high conductivity as compared to grain boundaries. Thus, dielectric constant decreases at high frequencies. Dielectric constant increases and tangent loss decreases (Fig. 3) up to a Bi/Fe ratio of 1.10. This increase in dielectric constant is associated with phase pure BiFeO$_3$ at Bi/Fe ratio 1.10. In addition, as crystallite size increases (Fig. 2) at Bi/Fe ratio 1.10, decrease in dislocation density and strain takes place. As a result of which, probability of the formation of 180˚ domain wall increases thus increasing dielectric constant (Shah et al. 2014a,b). In addition, an important factor that influences the dielectric constant and tangent loss is the presence of oxygen vacancies. Because of the presence of different phases at Bi/Fe ratios 0.9 and 1.20 hopping conduction mechanism in bismuth iron oxide increases. This increases the

probability of increase in number of oxygen vacancies. As oxygen vacancies increase dielectric constant decreases and tangent loss increases (Shah et al. 2014a,b).
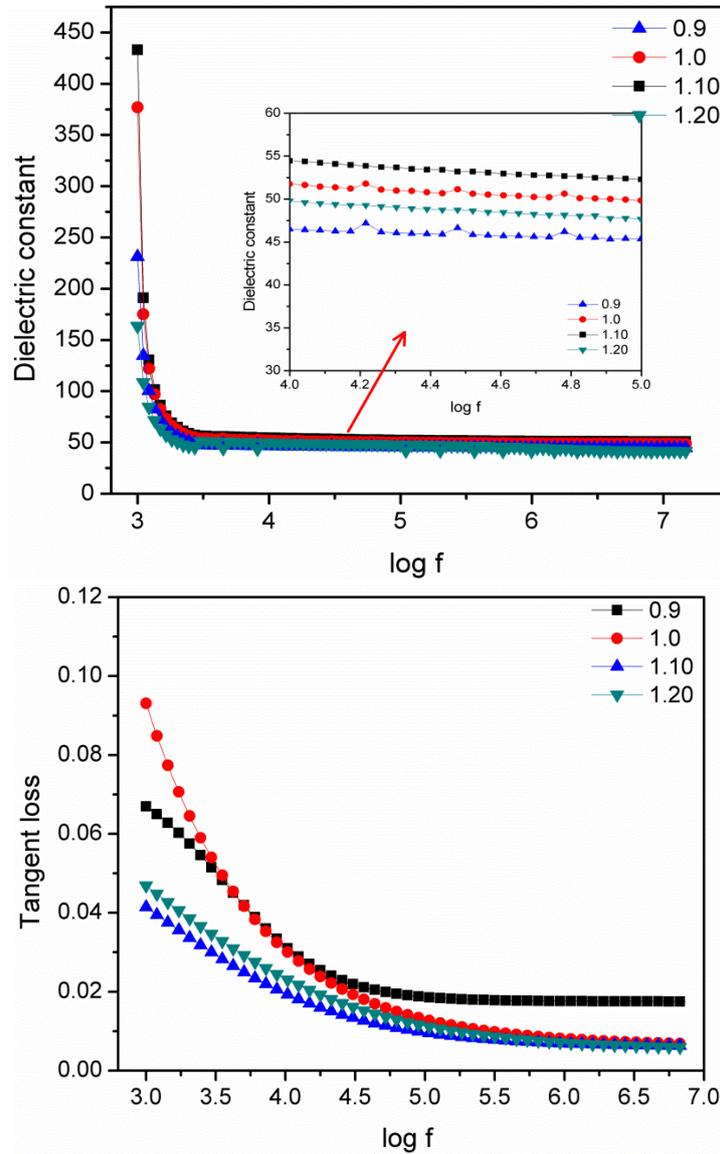

Fig 3. Dielectric constant and Tangent loss for $BiFeO_3$ thin films

Transmittance properties that are related to electronic structure and band gap have also been examined. Fig. 4 shows transmittance spectrum of bismuth iron oxide thin films with variation in Bi/Fe ratio as 0.9, 1.0, 1.10, and 1.20 in the range of 400nm and 1200nm. Transmittance in the visible and UV corresponds to fundamental absorption region for our films (Riaz and Naseem, 2015). With variation in Bi/Fe ratio to 1.0 and 1.10, transmission of the films increases. This increased transmission is associated with increase in crystallite size and decrease in dislocation density (Fig. 2). Increase in crystallite size leads to decrease in number of grain boundaries (Riaz and Naseem 2015). Grain boundaries act as scattering centers thus high transmission at

Bi/Fe ratio 1.10 is associated with increase in crystallite size. In optoelectronic devices bismuth iron oxide is important oxide material. Surface roughness and transparency are important parameters for the study of optical properties. Thin films are transparent over a large wavelength range and become absorbent at 480nm and shifts towards lower wavelength as ratio of Bi/Fe is varied.
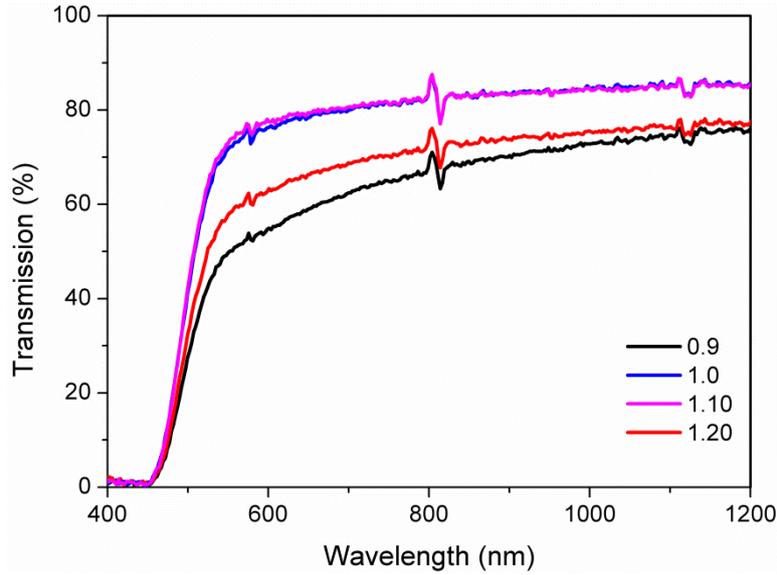

Fig 4. Transmission curves for $BiFeO_3$ thin films

Energy band gap of bismuth iron oxide thin films was calculated using the transmission curves and following Eq. 5.

$$\alpha = \frac{1}{t} \ln \left[\frac{2R^2 T}{-(1-R)^2 + \sqrt{(1-R)^4 + 4R^2 T^2}} \right] \tag{5}$$

Where, T is the transmission, R is reflection and t is thickness of the films. By plotting α^2 versus E (eV) in Fig. 5 direct band gap values can be observed by extrapolation of linear portions towards x-axis. From the plots, values of band gap are found to be in the range of 2.48-2.55eV. These values of band gap are in good agreement with the previously reported values. One possible tool to describe the band gap variation is the amount of oxygen vacancies. Oxygen vacancies within the band gap can form localized levels which result in the narrowing of band gap. So band gap reduction in bismuth iron oxide thin films at Bi/Fe ratio 0.9 and 1.20 is associated with presence of oxygen vacancies and mixed phases as observed in Fig. 1.
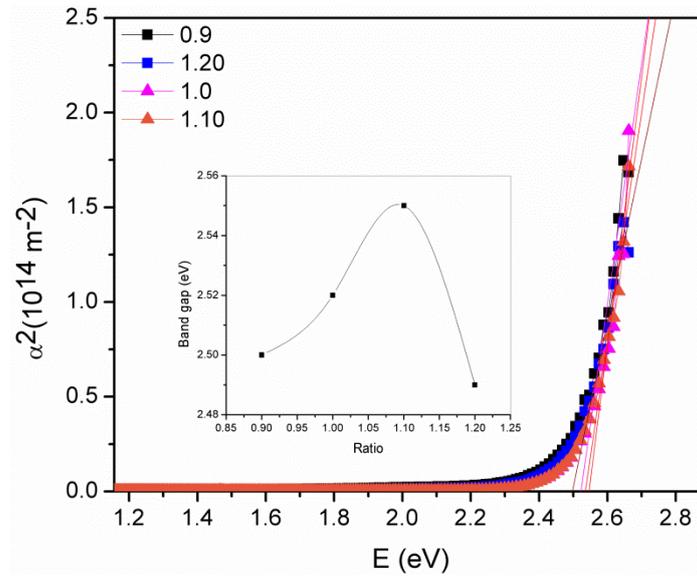
Fig 5. α^2 vs. E (eV) for BiFeO$_3$ thin films

Optical parameters such as refractive index and extinction coefficient were determined using Variable Angle Spectroscopic Ellipsometer (VASE). This is an indirect method and requires some mathematical model to monitor the changes in optical parameters. The model used in this study for bismuth iron oxide thin films was Cauchy model. Fig 6 shows increasing trend of refractive index. However decrease in refractive index is due to involvement of more oxygen vacancies in bismuth iron oxide lattice (Guo et al. 2102). High refractive index and low extinction coefficient for bismuth iron oxide thin films at Bi/Fe ratio 1.10 is associated with high density of the films. Extinction coefficient was small in the visible region and decreased in the infrared region. High values of refractive index show compact structure of thin films.
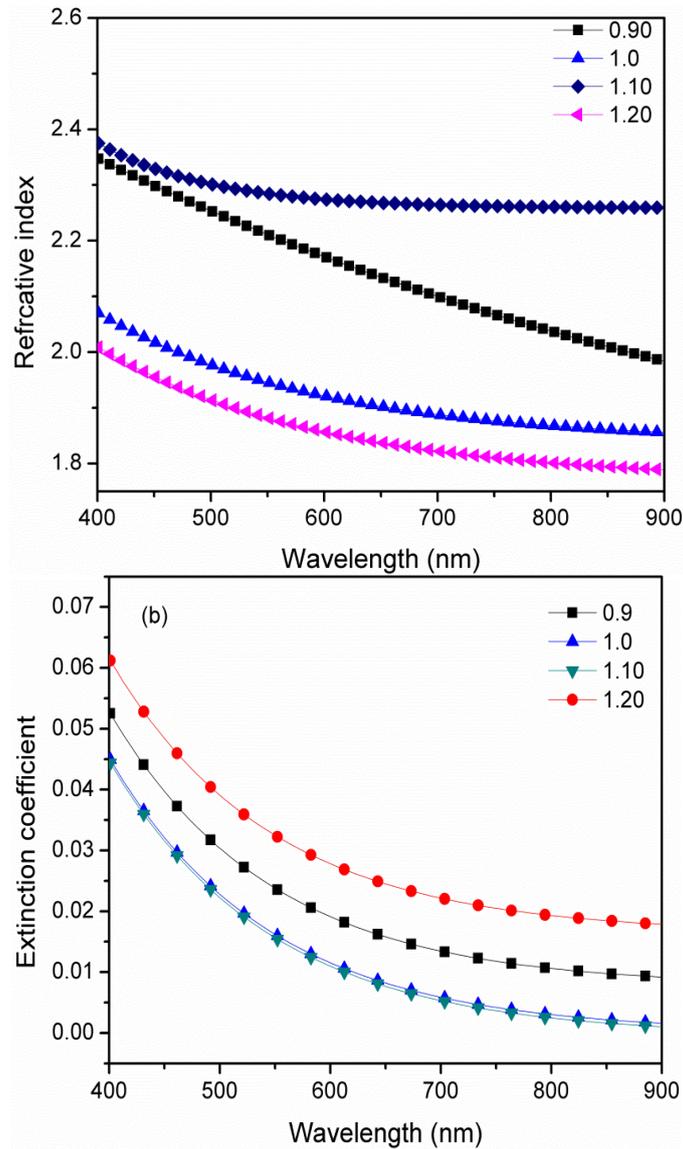
Fig 6. Refractive index and extinction coefficient for $BiFeO_3$ thin films

4. CONCLUSIONS

Thin films of bismuth iron oxide were prepared by sol gel and spin coating technique. Bi/Fe ratio was varied as 0.9, 1.0, 1.10 and 1.20. Phase pure bismuth iron oxide thin films were observed at Bi/Fe ratios of 1.0 and 1.10. Low Bi/Fe ratio i.e. 0.9 resulted in inclusion of bismuth deficient phase while high Bi/Fe ratio of 1.20 resulted in incorporation of bismuth rich phase. Crystallite size strongly depended on Bi/Fe ratio affecting the optical and dielectric properties of thin films. Dielectric constant increased and tangent loss decreased at Bi/Fe ratio of 1.10. High values of refractive index showed compact structure of these thin films. Direct band gap energy of the films was observed to be in the range of 2.48-2.55eV.

REFERENCES

Arora, M. Chauhan, S. Sati, P.C. and Kumar, M. (2014), "Effect of non-magnetic ions substitution on structural, magnetic and optical properties of $BiFeO_3$ nanoparticles", *J. Supercond. Nov. Magn.*, DOI 10.1007/s10948-014-2521-4.

Cullity, B.D. (1956), "Elements of x-ray diffraction," Addison Wesley Publishing Company, USA.

Fiebig, M. Lottermoser, T.H. Fröhlich, D. Goltsev, A.V. Pisarev, R.V. (2002), "Observation of coupled magnetic and electric domains", *Appl. Phys. Lett.*, **419**, 6909818–820.

Gao, R.L. Zhang, H.R. Fu, C.L. Cai, W. Chen, G. Deng, X.L. and Sun, J.R. (2016), "Transverse photovoltaic effect of tetragonal $BiFeO_3$ films", *J. Phys. Chem. Solids*, **92**, 32–37.

Guo, B. Guo, Y. (2012) "Optical properties of $BiFeO_3$–$(Na_{0.5}Bi_{0.5})TiO_3$ thin films deposited on glass substrates", *Mater. Lett.*, **71**, 241-254.

Ke, H. (2011), "Factors controlling pure-phase multiferroic $BiFeO_3$ powders synthesized by chemical co-precipitation", *J. Alloys Compd.*, **509**, 2192–2197.

Khomchenko, V.A. (2009), "Doping strategies for increased performance in $BiFeO_3$", *J. Magn. Magn. Mater.*, **321**,1692–1698.

Kumar, N. Sharma, V. Parihar, U. Sachdeva, R. Padha, N. and Panchal, C.J. (2011) "Structure, optical and electrical characterization of tin selenide thin films deposited at room temperature using thermal evaporation method", *J. Nano- Electron. Phys.*, **3**, 117-126.

Liu, H. Liu, Z. and Yao, K. (2007), "Improved electric properties in $BiFeO_3$ films by the doping of Ti" *J. Sol-Gel Sci. Technol.*, **41**, 2, 123–128.

Mazumder, R. Ghosh, S. Mondal, P. Bhattacharya, D.S. Dasgupta, S. Das, N. and Sen, A. (2006), "Particle size dependence of magnetization and phase transition near TN in multiferroic $BiFeO_3$," *J. Appl. Phys.*, **100**, 033908.

Riaz, S. Majid, F. Shah, S.M.H. and Naseem, S. (2014a), "Enhanced magnetic and structural properties of Ca doped $BiFeO_3$ thin films", *Indian J. Phys.,* **88**, 1037–1044.

Riaz, S. Shah, S.M.H. Akbar, A. Atiq, S. and Naseem, S. (2015), "Effect of Mn doping on structural, dielectric and magnetic properties of $BiFeO_3$ thin films", *J. Sol-Gel Sci. Technol.,* **74**, 310-319.

Riaz, S. Shah, S.M.H. Akbar, A. Kayani, Z.N. and Naseem, S. (2014b), "Effect of Bi/Fe ratio on the structural and magnetic properties of $BiFeO_3$ thin films by Sol-Gel", *IEEE Trans. Magn.* **50**, 2201304.

Salje, E.K.H. (1990), "Phase transitions in ferroelastic and co-elastic crystals", Cambridge Univ. Press, Cambridge.

Shah, S.M.H. Akbar, A. Riaz, S. Atiq, S. and Naseem, S. (2014a), "Magnetic, structural, and dielectric properties of $Bi_{1-x}K_xFeO_3$ thin films using Sol-Gel," *IEEE Trans. Magn.* **50**, 2201004.

Shah, S.M.H. Riaz, S. Akbar, A. Atiq, S. and Naseem, S. (2014b), "Effect of solvents on the ferromagnetic behavior of undoped $BiFeO_3$ prepared by Sol-Gel," *IEEE Trans. Magn.* **50**, 2200904.

Sharma, S. Saravanan, P. Pandey, O.P. Vinod, V.T.P. Cernik, M. and Sharma, P. (2016), "Magnetic behavior of sol–gel driven BiFeO$_3$ thin films with different grain size distribution", *J. Magn. Magn. Mater.*, **40**, 180–187.

Tripathy, S.N. Mishra, B.G. Shirolkar, M.M. Sen, S. Das, S.R. Janes, D.B. and Pradhan, D.K. (2013), "Structural, microstructural and magneto-electric properties of single-phase BiFeO$_3$ nanoceramics prepared by auto-combustion method", *Mater. Chem. Phys.*, **141**, 423-431.

Yan, J. Gomi, M. Hattori, T. Yokota, T. and Song, H. (2013), "Effect of excess Bi on structure and ferroelectric properties of polycrystalline BiFeO$_3$ thin films", *Thin Solid Films*, **542**, 150–154.

Zhao, J. Liu, S. Zhang, W. Liu, Z. and Liu, Z. (2013), "Structural and magnetic properties of Er-doped BiFeO$_3$ nanoparticles", *J. Nanopart. Res.,* **15**, 1969.

Zhao, S. (2014), "Enhanced ferromagnetism of cluster assembled BiFeO$_3$ nanostructured films", *Thin Solid Films*, http://dx.doi.org/10.1016/j.tsf.2014.02.031.